Radio Frequency Selective Addressing of Localized Atoms in a Periodic Potential

H. Ott, E. de Mirandes, F. Ferlaino, G. Roati, V. Türck, G. Modugno, and M. Inguscio

LENS and Dipartimento di Fisica, Università di Firenze, and INFM, Via Nello Carrara 1, 50019 Sesto Fiorentino, Italy

(Received 31 March 2004; published 16 September 2004)

We study the localization and addressability of ultracold atoms in a combined parabolic and periodic potential. Such a potential supports the existence of localized stationary states and we show that applying a radio frequency field allows us to selectively address atoms in these states. This method is used to measure the energy and momentum distribution of the atoms in the localized states. We also discuss possible extensions of this scheme to address and manipulate atoms in single lattice sites.

DOI: 10.1103/PhysRevLett.93.120407 PACS numbers: 03.75.Lm, 03.65.Ge, 03.67.–a

Periodic potentials have been used with great success in a series of experiments with ultracold atoms [1–4]. In most trapping geometries, the periodic potential is accompanied with an additional parabolic confinement [3,4]. For a Bose-Einstein condensate, the ground state is not dramatically modified by the parabolic potential. However, for the excited states of the system, the additional harmonic confinement must be taken into account. This is especially true for atomic Fermi gases, where the Pauli principle enforces a population of higher energetic states. The qualitative different nature of the single particle states can be seen from recent experiments with ultracold fermions, which have found evidence for a localization of the atoms in such a potential [5–7]. In the Mott insulating phase, the localization is due to the repulsive interaction [4]. Here instead, the phenomenon is a pure consequence of the potential shape. It is therefore important to understand its properties and physical consequences, nonetheless because the theoretical work on quantum phase transitions involving fermions [8–11] is mostly based on homogeneous systems [9–11]. A combined periodic and parabolic potential is also interesting for possible applications in quantum information and was recently proposed for the implementation of a qubit register for fermions [12]. A possible addressability of individual atoms in single lattice sites is thereby an intriguing vision.

In this Letter, we study ultracold atoms in a parabolic magnetic potential that is superimposed in its weak direction with a one-dimensional optical lattice. The combined potential possesses two distinct classes of eigenstates, which—depending on their energy—either extend symmetrically around the trap center or are localized on the sides of the potential. We use a radio frequency technique to address the atoms in localized states and to measure the density of states along the lattice direction as well as the momentum distribution of the atoms. Because of the localization, the radio frequency field addresses the atoms in a defined spatial region and we discuss the possibility of extending this scheme to manipulate individual atoms in single lattice sites.

In the experiment, we prepare an ultracold cloud of ^{87}Rb in the combined potential by forced evaporative cooling. The magnetic trapping potential has an axial and radial oscillation frequency of $\omega_a = 2\pi \times 16$ Hz and $\omega_r = 2\pi \times 197$ Hz, and the optical lattice ($\lambda = 830$ nm) can be adjusted between $0 < s < 10$, where s measures the potential height in units of the recoil energy $E_r = h^2/2m\lambda^2$. The atoms are prepared in the spin-polarized $|F = 2, m_F = 2\rangle$ state and the temperature is between 500 and 600 nK. Under these conditions, fermions would exhibit the same phenomenology like bosons as long as interparticle interactions can be neglected.

To understand the properties of the combined potential we first solve the 1D Schrödinger equation in the direction of the lattice,

$$\left[-\frac{\hbar^2}{2m}\frac{\partial^2}{\partial x^2}+\frac{1}{2}m\omega^2x^2+\frac{s}{2}E_r(1-\cos 4\pi x/\lambda)\right]\psi = E_n\psi, \tag{1}$$

where E_n is the energy of the nth eigenstate. This Hamiltonian has also recently been studied in tight binding approximation [13,14]. In Fig. 1(a), we show a density plot of the first 1000 eigenfunctions of (1). Each line in Fig. 1(a) corresponds to a density plot of the wave function. For low energies we find delocalized states that spread symmetrically around the potential minimum. Above a threshold energy, the wave functions of the eigenstates become localized on both sides of the potential. If we look at higher energies, a second group of eigenstates appears, centered again around the trap minimum. It is straightforward to identify this shell-like structure with the well-known band picture for a pure periodic potential. This becomes particularly clear if one looks at the accessible energy values for a given position which correspond to the calculated bandwidth E_{bw} and band gap E_{gap} of a pure sinusoidal potential, only shifted in energy by the local value of the parabolic potential. As a direct consequence, the system does not have an absolute but a spatially varying energy gap. The temperature of the cloud is chosen so that the bandwidth of the first band is much smaller than the average energy of the

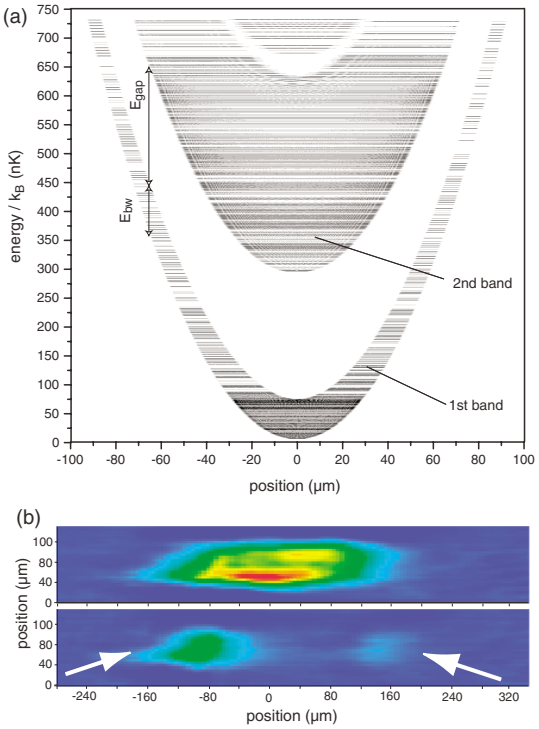

FIG. 1 (color online). (a) Spectrum of the Hamiltonian: representation of the 1D spectrum of the single particle Schrödinger equation for a combined parabolic and periodic potential with $s = 3$. Each line represents one eigenstate of the system, which is plotted as density profile in gray scale. The vertical position of the profile corresponds to the energy of the eigenstate. (b) Cloud of atoms without rf field (upper image), and with applied rf field (lower image) after 1.5 ms time of flight. The parameters of the rf field are $\nu_{up} = 632$ kHz, $\nu_{low} = 624$ kHz. The substructure in the upper cloud is due to the finite resolution of our imaging system.

atoms, thus providing a high population of the localized states. In the two radial directions, the atoms occupy the harmonic oscillator states.

We now introduce our experimental technique to prepare and address the atoms in the localized states. After the preparation of the atomic cloud in the combined potential, a radio frequency (rf) field is applied in order to induce spin flip transitions into Zeeman states which are not trapped by the magnetic radial confinement. Thus, atoms are removed from the potential if their wave function has a spatial overlap with the magnetic field shell defined by the resonance condition $h\nu = \mu_B B(\mathbf{r})/2$. Periodically sweeping (1 kHz rate) the radio frequency within an interval $\Delta\nu = \nu_{up} - \nu_{low}$, we define a spatial region in which the atoms are removed from the potential. After 100 ms we switch off the rf field together with the optical and magnetic potential and the cloud is imaged after 1.5 ms of free expansion [Fig. 1(b) lower image]. We observe two clouds of atoms, which are located at the sides of the potential [17]. These atoms are trapped in localized states and the result directly shows that the rf field is capable to address the atoms in a defined spatial region. For comparison, we show a cloud of atoms prepared under identical conditions but without applying the rf field [Fig. 1(b), upper image]. We have checked that (i) without the optical lattice all atoms are removed from the trapping potential and (ii) after switching off the rf field, the atoms remain on their position in the trap if the combined potential is kept on. Only for small lattice heights can we observe a slow motion of the two clouds towards the trap center. This is due to presence of collisions, which allow the bosons to hop between different localized states [6]. For a spin-polarized Fermi gas, this effect would be absent.

In our recent work [5–7], we were able to detect the localization of the atoms by looking at the center of mass position of the whole cloud. Here, we can employ this kind of rf spectroscopy to look at the energy distribution of the atoms in the localized states. In Fig. 2(a), we show a series of absorption images where we have scanned the rf field with a fixed frequency interval $\Delta\nu = 3$ kHz. Increasing the rf frequency, we start to remove atoms from the center of the trap. The hole in the spatial distribution deepens until the lower frequency bound is higher than the resonance frequency at the trap bottom: atoms in the center are no longer removed from the potential and we observe three clouds. For even higher frequencies the atoms are unaffected by the field and the two lateral clouds disappear. In Fig. 2(b), we show the number of atoms in the left cloud in dependence on the upper frequency of the rf field. Because of the localization, these atoms have an axial energy which is higher

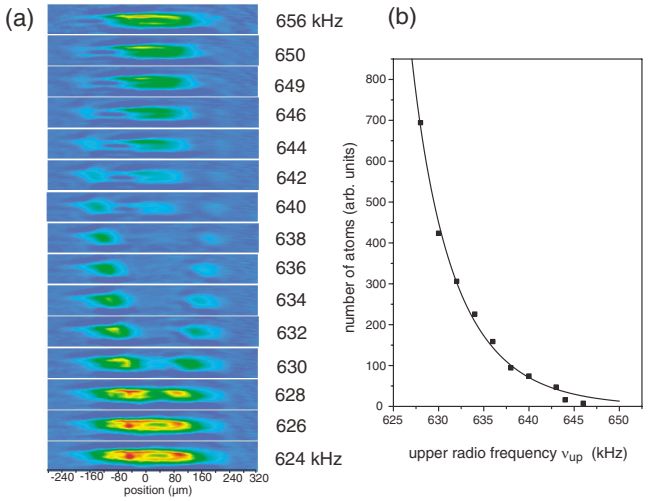

FIG. 2 (color online). Energy distribution of localized states in a lattice with $s = 9$. (a) Scan of the rf field through the cloud. The indicated frequencies are the upper frequency ν_{up} of the rf field; the sweep range of the rf field is 3 kHz. (b) Atom number in the left cloud in dependence on ν_{up}. The solid line is a fit with an axial density of states that is proportional to $E^{-1/2}$ (see text).

than $E_{up} = 2h(\nu_{up} - \nu_0)$, where ν_0 is the resonance frequency in the trap center. Thus, the number of atoms in the cloud is determined by the density of states in the axial direction: $N \propto \int_{E_{up}}^{\infty} n(E_a)\rho_a(E_a)dE_a$, where $\rho_a(E_a)$ is the density of states in the axial direction and $n(E_a) = e^{-E_a/k_B T}$ is the axial energy distribution. As shown in Refs. [13,14] the density of states for energies larger than the bandwidth of the first band is predicted to be proportional to $E^{-1/2}$. Using this value for $\rho_a(E_a)$, we fit our data with the above expression for N leaving the temperature and a constant of proportionality as free parameters [15]. The result, which is shown in Fig. 2(b), is consistent with our data.

We now turn to the momentum distribution of the localized states. For a potential depth of $s = 3$ we have calculated the Fourier transform of the wave functions of the eigenstates. Figure 3(a) shows the momentum distribution for selected eigenstates within the first and second band. The lowest eigenstate shows the well-known peak structure at multiples of twice the Bragg momentum. With increasing energy, these peaks broaden and develop a substructure. The momentum distribution of the localized states spreads nearly homogeneously over the first Brillouin zone ($\pm p_B$), independent of the energy of the state. Because the momentum distribution of the atoms in the radial direction is determined by the temperature of the ensemble, localized clouds as shown in Fig. 1(b) are expected to exhibit an anisotropic expansion. In Fig. 3(b) we show an absorption image of a localized cloud after 10 ms time of flight for $s = 3$ and $s = 9$. The measured aspect ratio of 2.5 for $s = 3$ reveals the strong anisotropy and proves the nonclassical momentum distribution of the localized states. For $s = 9$, the cloud expands much faster in the direction along the lattice (horizontal direction). Indeed, we calculate a 2 times larger momentum distribution for $s = 9$ with respect to $s = 3$ which leads to a nearly isotropic expansion.

We finish this work by discussing the localization process and its possible applications. For small lattice heights, the localization of the atoms is prevented by interband transitions. As an example, we show in Fig. 4(a) an excited state for $s = 0.3$ whose wave function exhibits substantial contributions from both bands. Consequently, an atom in this state is no longer confined within a single band. For increasing lattice height, the extension of the localized state shrinks [Fig. 4(b)] and approaches a minimum value which is given by the extension of the ground state in a single lattice site. For our

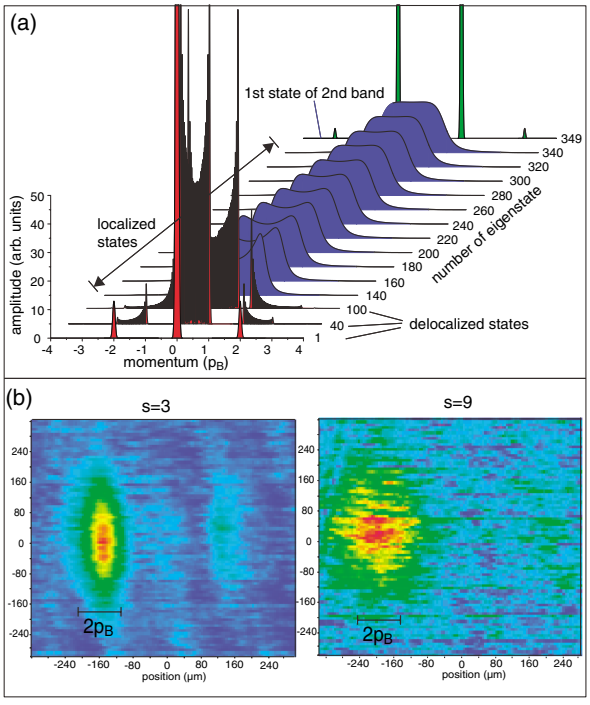

FIG. 3 (color online). Momentum distribution of the localized states. (a) Fourier transform of selected eigenstates of the spectrum shown in Fig. 1(a). The first three states are delocalized and lie within the first band; the last state is the first state of the second band. The states in between are localized states. (b) Absorption images of a cloud of atoms after application of the rf field for $s = 3$ and $s = 9$. To reveal the momentum distribution, the time of flight was chosen to be 10 ms.

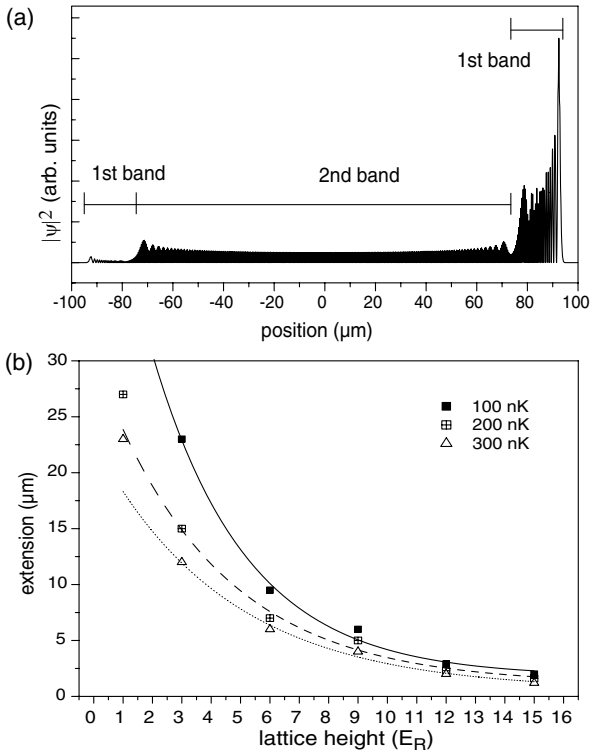

FIG. 4. (a) Tunneling between the bands: density distribution of the 594th eigenstate for a potential with $s = 0.3$. (b) Extension of the localized states in the first band in dependence on the lattice height for three different energies ($k_B \times 100$ nK, $k_B \times 200$ nK, and $k_B \times 300$ nK).

parameters we find that for $s = 30$, the eigenstates are mainly located within a single lattice site. This result is of particular interest because it shows that for similar experimental conditions like in the Mott insulator experiment [4], a localization of the atoms within one lattice site is possible without a repulsive interaction. Indeed, Viverit *et al.*[12] have shown that if an atomic Fermi gas is loaded in a combined parabolic and periodic potential, even an occupancy with exactly one atom per lattice site can be achieved. Another intriguing consequence of the localization is the addressability of single lattice sites: the potential gradient discriminates the resonance condition for an atomic transition in each lattice site if the transition depends on the external potential. In our setup, the magnetic potential leads to a spatially varying Zeeman splitting within the $|F = 2\rangle$-manyfold, and thus a very weak radio frequency should allow—in principle—for the manipulation of the atoms within one lattice site. To get a reasonable discrimination and a sufficiently high Rabi frequency, the resonance condition between adjacent lattice sites should be shifted by at least 10 kHz which would require a gradient of 300 G/cm [16]. For this purpose, a linear potential is more favorable than a parabolic one where the frequency shift is changing along the lattice. In order to achieve well-defined experimental conditions, it is also desirable to provide an optical confinement in the radial direction because otherwise, atoms with lower axial but higher radial energy can also be resonant with the radio frequency.

In conclusion, we have proved that atoms in a combined periodic and parabolic potential are trapped in localized states. We have used a radio frequency field to induce spatially resolved spin flip transitions in order to remove the atoms from the potential. This allowed us to measure the axial density of states and the momentum distribution of the localized states. The experiment has implications in various directions. First, it shows that an inhomogeneous periodic potential exhibits a qualitatively different phenomenology compared to a homogeneous system. Second, the experiment directly evidences a new localization mechanism which is a pure consequence of the potential shape. Especially for atomic Fermi gases, such a potential can be interesting to create single lattice site occupancy [12]. Third, we show that the atoms can be spatially addressed. For future experiments, it should be possible to extend the scheme to the manipulation of atoms in single lattice sites which would constitute a major progress in "quantum engineering" with ultracold atoms.

This work was supported by MIUR, by EU under Contract No. HPRICT1999-00111, and by INFM, PRA "Photonmatter." H. O. and V. T. were supported by EU under Contracts No. HPMF-CT-2002-01958 and No. HPMF-CT-2002-01649.

[1] M. Ben Dahan, E. Peik, J. Reichel, Y. Castin, and C. Salomon, Phys. Rev. Lett. **76**, 4508 (1996).
[2] S. R. Wilkinson, C. F. Bharucha, K. W. Madison, Qian Niu, and M. G. Raizen, Phys. Rev. Lett. **76**, 4512 (1996).
[3] F. S. Cataliotti, S. Burger, C. Fort, P. Maddaloni, F. Minardi, A. Trombettoni, A. Smerzi, and M. Inguscio, Science **293**, 843 (2001).
[4] M. Greiner, O. Mandel, T. Esslinger, T. W. Hänsch, and I. Bloch, Nature (London) **415**, 39 (2002).
[5] G. Modugno, F. Ferlaino, R. Heidemann, G. Roati, and M. Inguscio, Phys. Rev. A **68**, 011601(R) (2003).
[6] H. Ott, E. de Mirandes, F. Ferlaino, G. Roati, G. Modugno, and M. Inguscio, Phys. Rev. Lett. **92**, 160601 (2004).
[7] L. Pezzé, L. Pitaevskii, A. Smerzi, S. Stringari, G. Modugno, E. de Mirandes, F. Ferlaino, H. Ott, G. Roati, and M. Inguscio, Phys. Rev. Lett. (to be published).
[8] M. Rigol, A. Muramatsu, G. G. Batrouni, and R. T. Scalettar, Phys. Rev. Lett. **91**, 130403 (2003).
[9] A. Albus, F. Illuminati, and J. Eisert, Phys. Rev. A **68**, 023606 (2003).
[10] H. P. Büchler and G. Blatter, Phys. Rev. Lett. **91**, 130404 (2003).
[11] M. Lewenstein, L. Santos, M. A. Baranov, and H. Fehrmann, Phys. Rev. Lett. **92**, 050401 (2004).
[12] L. Viverit, C. Menotti, T. Calarco, and A. Smerzi, Phys. Rev. Lett. **93**, 110401 (2004).
[13] M. Rigol and A. Muramatsu, Phys. Rev. A (to be published).
[14] C. Hooley and J. Quintanilla, Phys. Rev. Lett. **93**, 080404, (2004).
[15] The x-axis in Fig. 2(b) is not directly the energy in the potential because our trap bottom exhibits long term drifts. As the different data points were taken in time order a linear drift leads to a scaling of the energy axis which can be compensated by leaving the temperature in the fitting procedure as a free parameter.
[16] For this gradient, the required lattice height for a localization within one lattice site and a simultaneous suppression of Zener tunnelling is $s > 10$.
[17] The asymmetry in the population of the two clouds rises from a small horizontal tilt of our magnetic trap with respect to gravity. As a consequence, the potential minimum does not coincide with the magnetic field minimum.